MULTIVARIABLE OPTIMIZATION OF CYCLING BIOMECHANICS

M. L. Hull, Ph.D.
Department of Mechanical Engineering
University of California

Hiroko Gonzalez, MS
Department of Mechanical Engineering
University of California

NOMENCLATURE

x,y,z	Denote axes of inertial coordinate system with x-y in the plane of the bicycle.
$P,\bar{P}$	Instantaneous and average power respectively.
F_n	Component of resultant pedal force vector driving the crank.
$\theta,\dot{\theta},\ddot{\theta}$	Angular position, angular velocity, and angular acceleration of the crank arm respectively (from vertical, clockwise).
T	Time to complete one crank revolution.
L_c,L_f,L_s,L_t	Lengths of the crank arm, foot, shank and thigh respectively.
L1	Crank arm length.
L2i	Longitudinal foot position on the pedal.
L5	Seat height (measured from crank spindle axis to hip axis).
Ψ	Seat tube angle (the angle between the seat tube and the horizontal axis).
$\alpha,\dot{\alpha},\ddot{\alpha}$	Angular position, angular velocity, and angular acceleration of the foot relative to the crank arm (clockwise).
$\beta,\dot{\beta},\ddot{\beta}$	Angular position, angular velocity, and angular acceleration of the foot (from horizontal, clockwise).
$\phi,\dot{\phi},\ddot{\phi}$	Angular position, angular velocity, and angular acceleration of the shank (from horizontal, counterclockwise).
$\gamma,\dot{\gamma},\ddot{\gamma}$	Angular position, angular velocity, and angular acceleration of thigh (from vertical, counterclockwise).
c,f,s,t,b	Denote links corresponding to crank, foot, shank, thigh and bicycle respectively.
o,p,a,k,h	Denote axes of rotation of crank spindle, pedal spindle, ankle, knee, and hip respectively.
PF_x,PF_y	Horizontal and vertical pedal force components respectively.
I_f,I_s,I_t	Centroidal moments of inertia of the foot, shank, and thigh respectively.
CG_f,CG_s,CG_t	Center of gravity distances of foot, shank, and thigh from proximal joint.
A_f,A_s,A_t	Absolute accelerations of the center of gravity of the foot, shank, and thigh respectively.
N	Number of equation solutions over a crank cycle.
M_a,M_k,M_h	Ankle, knee and hip moments respectively.
MCF	Moment Cost function.
m_f,m_s,m_t	Mass of the foot, shank and thigh respectively.
F_a,F_k,F_h	Forces at the ankle, knee, and hip respectively.

Introduction

In an activity of conventional cycling where the pedal travels a circular path at constant velocity, a number of variables affect the intersegmental loads in the leg when the power output is constant. As depicted in Figures 1a and 1b, four geometric variables are crank arm length, seat height, seat tube angle, and longitudinal foot position on the pedal. Considering the leg-bicycle to be a five-bar linkage constrained to plane motion (see Figure 2a), it is clear that each of these geometric variables influences the linkage kinematics and hence the intersegmental loads. Because of this influence these variables are termed biomechanical variables. In addition to the four geometric variables, a fifth biomechanical variable is the pedaling rate. Since these variables affect cycling biomechanics and are readily adjusted by a cyclist setting up his equipment, it is useful to determine a method for establishing optimum adjustments.

To identify optimum adjustments, the effect of all the above variables on some performance measure has been studied by previous researchers. Two basic approaches have been taken in such studies, human performance testing and analytical optimization analysis. One measure in human performance testing has been oxygen uptake. In the aerobic regime, oxygen uptake as a function of pedaling rate at constant power has been studied by Seabury et al. (1977), Faria et al. (1982), and Coast and Welch (1985). The results generally indicate that the optimum pedaling rate (i.e. the one resulting in minimum uptake) increases with workload and for a workload of 200W the optimum rate is 60 - 65 RPM. Also, oxygen uptake as a function of seat height has been studied by Hamley and Thomas (1967) and Nordeen-Snyder (1977). Both studies concluded that the uptake is minimized at a height of 100 percent of trochanteric leg length. Trochanteric leg length is the distance from the floor to the greater trochanter measured when a subject stands upright.

Another measure in human performance testing has been maximum power output. This measure was used by Harrison (1970) who examined the effect of crank arm length on maximum power production and concluded that length was relatively unimportant.

In analytical optimization analyses, performance measures take the form of objective (cost) functions which then must be either minimized or maximized. Miller and Ross (1980) relied on a mechanical impedance-based objective function to design a maximum power bicycle drive. However, this drive does not fall within the conventional cycling

definition given earlier since the velocity of the pedal is not constant over the crank cycle. More recently, Redfield and Hull (1986a) optimized pedaling rate using a joint moment-based objective function. They found that the optimal rate was in the range of 90-105 RPM at a power output level of 200W. This range agrees well with that naturally chosen by cyclists generating that power level.

Following the lead of Redfield and Hull (1986a), Hull et al. (1988) also optimized pedaling rate using a muscle-stress based cost function. This function was shown by Redfield and Hull (1986b) to better model the biomechanics of the leg than the joint moment-based cost function. The optimal pedaling rate found by Hull et al. (1988), however, was the same as that reported by Redfield and Hull (1986a). Hull et al. (1988) concluded that since optimization results were not significantly different for the two cost functions, it is advantageous to use the moment-based cost function in future analyses since it is simpler to compute.

One of the advantages of optimization analysis over human performance testing is ready capability of handling multi-variables. Such capability is important in optimization of cycling biomechanics since at least five variables must be considered. Broaching the subject of multivariable optimization, Hull and Gonzalez (1988) completed a two-variable optimization of pedaling rate and crank arm length using the joint moment based cost function. The sensitivity of the cost function to both variables was significant and the variables were interacting. The significance of the remaining variables to the cycling biomechanics optimization problem remains unknown, however.

The purpose of this study is to extend the optimization analysis to three, four and five variables, in order to understand the relation among all biomechanical variables and the intersegmental moments. The first objective is to examine the sensitivities of each of the five variables. The hypothesis is that all of the five biomechanical variables listed above significantly affect the joint moment-based cost function when allowed to vary over a practical range. The second objective is to simplify the optimization problems by reducing the number of variables if any are noninteracting (Pierre, 1969). A third objective is to solve the multivariable optimization problem where all five variables are considered simultaneously. The solution will determine if a set of variable values exists such that the joint moment-based cost function is minimized while all variable values are within practical limits.

A further objective stems from examining the equations of

Redfield and Hull (1986a) governing the motion of the lower limb model in cycling. Among the input data necessary to solve these equations are a variety of anthropometric parameters. The solution will depend to some degree on these parameter values. Recognizing that the anthropometry of the rider will affect optimization results, a fourth objective is to assess this influence on the results.

Finally, considering that the study of bicycling biomechanics is performed at a constant power output level, pedal force-time histories must be scaled when either the length of the crank arm L_c, or the angular velocity (i.e., pedalling rate), o, is varied, in order to maintain a constant average power output. The necessity of this scaling is apparent from the relation between power and these two variables. The instantaneous power P developed about the crank spindle is given by

$$P = F_n L_c \dot{\theta} \qquad (1)$$

where F_n is the component of the resultant pedal force perpendicular to the crank arm, and F_n is computed from the horizontal and vertical pedal force components, PF_x and PF_y respectively. Thus, a final objective is to check that the scaling method adopted herein yields pedal force profiles representative of those measured when the pedaling rate is varied at constant power.

Methods

The leg-bicycle system was modeled as a planar five-bar linkage fixed at both the hip joint and crank axis (Figure 2a). Because the model is a five-bar linkage, it has two degrees of freedom. Therefore, to completely constrain the model, six kinematic inputs and one geometric constraint were needed. Derived from the work of Hull and Jorge (1985) the kinematic inputs were the experimentally acquired angular position (θ), velocity ($\dot{\theta}$) and acceleration ($\ddot{\theta}$) of the crank and the angular position (α), velocity ($\dot{\alpha}$) and acceleration ($\ddot{\alpha}$) of the foot link relative to the crank. As the geometric constraint, the knee joint was not allowed to extend past the straight leg position. Both the crank angle and the relative pedal angle with respect to the crank were measured experimentally using continuous rotation potentiometers. The crank angular velocity was held constant using a "paceometer" (a bicycle tachometer) and thus crank angular acceleration was zero. The relative pedal angle was determined to be sufficiently approximated by a sine function. Thus, the relative angular velocity and acceleration were found by analytically

differentiating the angle function. The justification for the sinusoidal approximation of the pedal angle is detailed in the paper of Redfield and Hull (1986a).

To determine the kinetics of the model, free body diagrams (Figure 2b) of each link were constructed and the equations of motion were written using Newton's Laws. In the notations of Figure 2a and 2b, the moment equations for each joint become:

$$\text{Ankle: } M_a = -I_f\ddot{\beta} + m_f[A_{fx}\,CG_f\,\sin\beta + A_{fy}\,CG_f\,\cos\beta] + m_f\,g\,CG_f\,\cos\beta + L_f\,PF_y\,\cos\beta + L_f\,PF_x\,\sin\beta \quad (2)$$

$$\text{Knee: } M_k = M_a + I_s\ddot{\phi} + m_s\,[A_{sx}\,CG_s\,\sin\phi - A_{sy}\,CG_s\,\cos\phi] + F_{ax}\,L_s\,\sin\phi - F_{ay}\,L_s\,\cos\phi - m_s\,g\,CG_s\,\cos\phi \quad (3)$$

$$\text{Hip: } M_h = M_k + I_t\ddot{\gamma}_3 + m_t[A_{tx}\,CG_t\,\cos\gamma_3 + A_{ty}\,CG_t\,\sin\gamma_3] + F_{kx}\,L_t\,\cos\gamma_3 + F_{ky}\,L_t\,\sin\gamma_3 + m_s\,g\,CG_t\,\sin\gamma_3 \quad (4)$$

The above relations indicate the need to specify values of anthropometric parameters. Segment lengths were estimated from Drillis and Contini (1966). Masses, moments of inertia about the center of gravity, and center of gravity locations were estimated using the data cited in Wells and Luttugens (1976). These parameters were estimated for three different sized people, the reference or average man who was 177.8 cm (5 ft. 10 in.) tall and weighed 72.5 kg (160 lbs), the short man who was 162.6 cm (5 ft. 4 in.) tall and weighed 58.9 kg (130 lbs.), and finally the tall man who was 193.0 cm (6 ft. 4 in.) tall, and weighed 90.6 kg (200 lbs). Table 1 lists the values of the anthropometric parameters for the three men.

Table 1 Values of Anthropometric Parameters

Average man: 72.5kg, 177.8cm

	Foot*	Shank	Thigh
Length(cm)	16.1	43.6	43.6
Mass(kg)	0.98	3.04	6.86
Moment of inertia about CG(kg-m^2)	2.3×10^{-3}	42.2×10^{-3}	69.0×10^{-3}
Distance of CG from proximal joint(cm)	6.9	18.9	18.9

Short man: 58.9kg, 162.6cm

	Foot*	Shank	Thigh
Length(cm)	14.9	39.9	39.9
Mass(kg)	0.80	2.47	5.57
Moment of inertia about CG(kg-m^2)	1.60×10^{-3}	28.7×10^{-3}	46.9×10^{-3}
Distance of CG from proximal joint(cm)	6.4	17.3	17.3

Tall man: 90.6kg, 193.0cm

	Foot*	Shank	Thigh
Length(cm)	17.4	47.4	47.4
Mass(kg)	1.22	3.81	8.57
Moment of inertia about CG(kg-m^2)	3.3×10^{-3}	62.4×10^{-3}	101.9×10^{-3}
Distance of CG from proximal joint(cm)	7.5	20.5	20.5

*Length given for foot is the link length in the five-bar linkage model.

Prior to solving the equations of motion, additional input data were necessary. First the pedalling rate and geometric variables were assigned values. Then in order to maintain constant average power over a complete crank revolution, the pedal force time histories were scaled. To understand the scaling, consider that the average power $\bar{P}$ is computed according to where T is the time to complete one crank revolution. The pedal force component F_n normal to the crank arm is related to the horizontal (PF_x) and vertical (PF_y) pedal forces by

$$\bar{P} = \frac{1}{T} \int_0^T F_n L_c \dot{\theta} dt \qquad (5)$$

Both pedal forces were measured by Hull and Jorge (1985) using a six-axis pedal dynamometer during the same experiments used to record the kinematic data. According to Eq. (5), variation of either the crank arm length L_c or the pedaling rate $\dot{\theta}$ requires an inverse variation in

$$F_n = (PF_x \cos\theta - PF_y \sin\theta) \qquad (6)$$

F_n to maintain constant average power. This inverse variation was achieved by scaling both measured pedal forces. Pedal forces were scaled so that Eq. (5) yielded 100W. Since this is a single pedal power level, the total power output is 200W (0.27 Hp).

With the input data specified, the equations of motion were solved starting with the foot and proceeding through each link to the thigh. Because the equations were solved over a complete crank cycle at 5 degree intervals, the solution yielded functional relations between the three joint moments and the crank angle (Eqs., (2), (3) and (4). Derived from the knee and hip moments, a joint moment cost function was defined as

$$MCF = \sum_{i=1}^{N} [(M_{ki}^2) + (M_{hi}^2)] \qquad (7)$$

where N is the number of data points and M_k, M_h are the knee and hip moments respectively. As described in the earlier article of Hull and Gonzalez (1988), this cost function is physiologically based in that joint moments are directly related to muscle stresses. Further squaring the moments (i.e. stresses) reflects the observation that muscle fatigue is related to muscle stress raised to a power between the 1.5 and 5 (Crowninshield and Brand, 1981). The rationale behind including only hip and knee moments in the cost function is that from experience, fatigue of the thigh muscles limits cycling performance. Finally, while the cost function defined by Eq. (7) has a physiological basis, it is not the only possible function which could be defined with such a basis. Alternative approaches to defining cost functions are discussed by Hull and Gonzalez (1988).

The analysis proceeded in five stages with the first being devoted to the sensitivity study. In all stages except for the fifth, the power level was adjusted to 100W (single leg), the power level chosen to be representative of steady state cruising cycling over flat terrain at 9 m/s (20 MPH). The anthropometric parameters were assigned values of the average man for the first three stages and of different size riders for the fourth and fifth stages.

The first stage began by defining a reference set of variable values for fixed anthropometry and then computing the cost function as each variable assumed values throughout its practical range. For the average man a reference value for each of the variables is defined as: 90 RPM for the pedaling rate, 0.170m for the crank arm length, 73° for the

seat tube angle, 0.784m for the seat height, and 0.125m for the longitudinal foot position on the pedal. The pedaling rate was chosen due to the fact that cyclists typically spin at about 90 RPM in cruising situations at the 200W power level (Whitt and Wilson, 1982). The crank arm length of 170mm is the industry standard. From the results of Hamley and Thomas (1976) and Nordeen-Snyder (1977) which showed that the seat height corresponds to 100 percent of the trochanteric leg length, the seat height is adjusted to this length for the average man. Next, the longitudinal foot position on the pedal is the horizontal distance from the ball of the foot to the ankle axis. The foot size for the average man was determined as 26.7 cm (size 9 1/2) (Drillis and Contini, 1966), and the longitudinal foot position on the pedal of 0.125m was measured from a subject with this size foot.

The objective of the first stage was to investigate the sensitivity of each of the five variables. In order to assess the relative degree of influence each variable has on the cost function, the cost function was normalized to its reference value and plotted against each of the five variables also normalized to their reference values. The first investigation was at the original reference point, and our other investigations were made at different points in 5-space to check the dependence of sensitivity on location in the space.

Before proceeding with the solution of the various optimization problems, the objective of the second stage was to simplify the optimization problems if possible by reducing the variable number. Reducing the number of variables is possible if any are noninteracting. To examine for noninteraction, consecutive one-dimensional searches were done for each variable about a specific point in n-space (n=3,4,5), and then the searches about a different specific point were repeated. If any of the variables were noninteracting, then the minimum identified in the two separate searches would be the same.

Guided by the results of the interaction analysis, the objective of the third stage was to solve a series of three optimization problems with increasing dimension from three to five. The purpose of this was to obtain a set of variable values such that the cost function was minimized and that all variable values were within practical limits. The variables chosen for the three-dimensional problem were those with the greatest sensitivity. A similar rationale served for the four-dimensional problem.

Because the third stage of analysis entailed solving three optimization problems of different dimension, it was necessary to

establish both variable ranges and fixed values for each problem. These are given in Table 2. The first problem was the three-dimensional optimization, where the seat height (L5) and the longitudinal foot position on the pedal (L2i) were fixed at the reference values of 0.784m and 0.125m respectively. The variable ranges for the three optimized variables, pedaling rate, crank arm length, and seat tube angle, extend above and below the reference values out to what are considered to be practical limits. In the second problem, the four-dimensional optimization, the variable range from 0.684m to 0.804m for seat height (L5) was added. The assignment of the seat height variable range was somewhat limited due to the γ_2 angle limitation; the knee joint could not extend beyond the thigh and shank being in a straight line. The five-dimensional optimization was the third problem, and the longitudinal foot position on the pedal (L2i) was allowed to vary from 0.104m to 0.143m. Allowing about ± 2 cm of variation from the reference, these limits are more generous than the ± 1 cm of adjustment which is the maximum offered by commercial cycling shoes.

The algorithm used for the multidimensional optimization problems is based on Powell's method. This method is well suited for this application because it gives quadratic convergence without the need to compute derivatives (Pierre, 1969). The software, which implemented this algorithm, is the IMSL Library routine, ZXMWD. The optimization routine would allow the global minimum to be predicted within the given variable ranges regardless of the contour shape.

The objective of the fourth stage was to examine if variable values minimizing the cost function were strongly dependent on anthropometric parameter values. Similar to the third stage, a series of three optimization problems with increasing dimension for two different size riders, the short man and the tall man (see Table 1), was solved in the practical range of variable values for each rider.

Some of the variable ranges were independent of anthropometry while some were dependent. The two that were independent were the cadence and the seat tube angle which ranged form 60 RPM to 140 RPM and 63° to 83° respectively. The other three variables were dependent on anthropometry because of changes in body segment lengths. Table 2 gives these ranges.

Table 2 Parameter Ranges for Different Size Riders

	Short man	Average man	Tall man
Cadence	60 RPM-140 RPM	60 RPM-140 RPM	60 RPM-140 RPM
Crank arm length (L1)	0.140 m-0.180 m	0.140 m-0.200 m	0.140 m-0.200 m
Seat tube angle (ψ)	63° - 83°	63° - 83°	63° - 83°
Seat height (L5)	0.548 m-0.739 m	0.684 m-0.804 m	0.736 m-0.876 m
Foot position on pedal (L2i)	0.089 m-0.130 m	0.104 m-0.143 m	0.115 m-0.156 m

The final stage was to examine the assumption of the pedal force scaling method. With the use of the two-load component pedal dynamometer of Newmiller and Hull (1986), pedal force profiles of an average size rider (height 1.77m, weight 71.1kg) were measured at 60 RPM to 120 RPM in 10 RPM increments. The experimental procedure called for having the test subject pedal at the various rates on a stationary Schwinn Velodyne electrically braked cycle ergometer. Similar to a standard wind trainer, the ergometer accepts the subject's own bicycle sans front wheel. The ergometer offers several modes of operation including a constant power mode used in this study. In this mode, the power required to drive the device is independent of the pedaling rate. The power level was set so that the average power for the single leg under study was 90W. Selected pedaling rates were set using a metronome. The test subject pedaled while using toeclips with cleats mounted on cycling shoes.

The experimental pedal force profiles were compared with the pedal force profiles calculated using the pedal force scaling method. The pedal force profiles at the median cadence of 90 RPM served as the reference from which scaled profiles were computed. The comparison was made by plotting pedal force versus crank angle for each cadence, for the experimental case, and for the pedal force scaling computational case, to examine the pedal force profiles qualitatively. The other comparison was done by calculating the moment cost function values for both cases in order to compare them quantitatively.

Results and Discussion

The results of the first stage of the analysis are illustrated in Figure 3. Recall that this stage was concerned with variable sensitivity. The moment-based cost function normalized to its reference value is plotted against the each of the five variables also normalized to their reference values. All variables except for the seat height were varied ±10 percent from their reference values. The seat height increase was constrained to +5 percent maximum because greater increases would necessitate knee hyperextension. From the figure, the sensitivity rankings become the following: the pedaling rate (the most sensitive), the crank arm length, the seat tube angle, the seat height, and the longitudinal foot position on the pedal (the least sensitive). The seat tube angle and height have a similar degree of sensitivity because both variables affect the horizontal and vertical seat height necessary for calculation of joint moments (see Figure 2a). Similar ordering and degree of sensitivity to the original reference point were observed at the four other points. Overall the results of the sensitivity analysis indicate that all of the five variables except foot position are sensitive enough to warrant attention in the multivariable optimization.

To obtain the results of the second stage, which was to simplify the optimization problems, the sensitivity profile plots were also inspected for possible noninteracting variables. Recall that if any of the variables are noninteracting, then the minima for a particular variable will be the same for separate one-dimensional searches made from two different points in the variable space. Figure 4 plots the sensitivity profiles of all five variables at one of the other four points. Comparing the minimum in Figure 4 to the minimum in Figure 3 for a particular variable shows that the minima in these two separate searches are not the same for any of the variables. Thus, all five variables are interacting so that the number of variables cannot be reduced.

The results of the three optimization problems with increasing dimension from three to five are listed in Table 3. These results imply that cyclists will minimize the cost function by setting the biomechanical variable values to the optimal variable values listed in the Table. The optimal variable values, however, especially for cadence and crank arm length, are high and short respectively relative to the standard of practice. From Figure 5, it is apparent how variations in crank arm length and cadence increase the minimum cost function value over the value corresponding to the global minimum. A crank arm length of 0.170m and cadence of 100 RPM increase the function

value by 4.0 percent. Recall the industry standard is 0.170m for crank length, and cyclists typically spin at about 90 RPM in cruising situations at the 200W power level; thus the global minimum obtained is about 4.0 percent less than the cost function value corresponding to the industry standard.

The fourth stage of the analysis was concerned with how variations in anthropometric parameters influence the results of the optimization analyses. Table 2 lists the variable ranges while Table 3 gives the results in three to five dimensions for both the short size man and tall size man (see Table 1). In examining the results in Table 3, note that the moment cost function values at the global minimum increase with size. As explained in detail in Hull and Jorge (1985), the total moment at each joint is the superposition of the static and kinematic moment contributions. The static contribution is the moment due to pedal forces only while the kinematic contribution is the moment due to motion of the leg only. The increase in the cost function minimum with size occurs because a taller man requires greater kinematic joint moments than others to move the crank due to the increased mass and moments of inertia of this larger lower limb segments.

Table 3 Optimum Variable Values of Global Minimum for Anthropometric Variations

	Short man	Average man	Tall man
Three dimensional optimization results:			
Cadence	117 RPM	107 RPM	98 RPM
Crank arm length (L1)	0.150 m	0.152 m	0.154 m
Seat tube angle (ψ)	78.1°	75.8°	73.3°
Ref. seat height (L5)	0.704 m	0.784 m	0.866 m
Ref. foot position (L2i)	0.114 m	0.125 m	0.136 m
Moment cost function value	40,146 N^2m^2	47,884 N^2m^2	57,607 N^2m^2

Table 3 Optimum Variable Values of Global Minimum for Anthropometric Variations

Four dimensional optimization results:			
Cadence	123 RPM	112 RPM	100 RPM
Crank arm length (L1)	0.140 m	0.143 m	0.150 m
Seat tube angle (ψ)	78.3°	75.8°	73.3°
Seat height (L5)	0.739 m	0.804 m	0.876 m
Ref. foot position (L2i)	0.114 m	0.125 m	0.136 m
Moment cost function value	38,687 N^2m^2	46,929 N^2m^2	57,071 N^2m^2
Five dimensional optimization results:			
Cadence	124 RPM	115 RPM	102 RPM
Crank arm length (L1)	0.140 m	0.140 m	0.148 m
Seat tube angle (ψ)	78.3°	75.7°	73.2°
Seat height (L5)	0.737 m	0.804 m	0.876 m
Foot position (L2i)	0.130 m	0.143 m	0.156 m
Moment cost function value	37,908 N^2m^2	45,809 N^2m^2	55,784 N^2m^2

Note now that the optimal crank arm lengths increase as the size of man increases. Even though all the optimal crank arm lengths tend to be less than the standard length, 0.170m, the results coincide with Borysewics (1985) who recommends that a taller man needs a longer crank arm than a shorter man and an average man.

Note also that as crank arm length increases, cadence decreases as the rider's size increases. Referring to Eqs. (1) and (5) provides some insight into how these variables affect joint moments. On the one hand, a longer crank arm length demands low pedal forces with the result that the static moments decrease. On the other hand, a longer crank arm length requires more motion from leg segments, which leads to an increase in the kinematic moments. However, a high RPM causes the kinematic moments to increase while the static moments decrease as indicated in Redfield and Hull (1986a). It is clear that crank arm length and pedaling rate effects are opposite. Evidently, when the effects are superimposed, the trends regarding anthropometry in Table 3 are obtained.

Next, Table 3 indicates that the seat tube angle decreases as the rider size increases. When the angle decreases, the location of the hip axis shifts backward relative to the crank axis. The trend between seat tube angle and anthropometry is difficult to interpret because of the complex relationship between this angle and leg geometry at a given crank angle. The results indicate that a taller man whose leg segments are larger will benefit from shifting position rearward of that of the average man while a shorter man whose leg segments are smaller will benefit from shifting his position forward.

The other two variables also exhibit trends due to anthropometric parameter variations. Both the seat height and the longitudinal foot position on the pedal increase as the size of rider increases. Regarding the seat height, although the absolute height changes, the relative height is consistent. When the sum of the crank arm length and the seat height is compared with the 100 percent trochanteric leg length for each size man, the sum of the optimal variable values is 2 percent to 3 percent less than the corresponding trochanteric leg length for the three different men. This implies that the riders benefit from adjusting their seat heights to 97 - 98 percent trochanteric leg lengths. The optimal seat height identified here agrees closely with that of Hamley and Thomas (1967) who used minimum oxygen uptake as the criterion for identifying the optimal height.

Similar to seat height, the longitudinal foot position increases with rider size. The optimal variable values for the foot position are all at maximum lengths of the practical range. Referring to Eqs. (3) and (4), notice that the ankle moment contributes to calculation of the knee and hip moments. Even though the ankle moment increases when the longitudinal foot position length on the pedal is increased, the superposition with other terms in Eqs. (3) and (4) gives a lower moment cost function result. This indicates that riders benefit from positioning their foot further back on the pedal.

Since the optimum foot positions are at maximum lengths, the question arises as to whether further increases in foot position would produce further reduction in the cost function minimum. Given the interpretation above to account for the foot position results, such a reduction seems likely. Thus a search for the optimum foot position that minimizes the cost function without any limiting constraints may be of interest despite the impracticality of the results. However, due to a limitation of the computer algorithm in handling a greater variable

range, this search could not be made.

The result that the pedaling rate and crank arm length are higher and shorter respectively than the standards of practice is consistent with Hull and Gonzalez (1988) who limited their optimization analysis to these two variables. Hull and Gonzalez gave a detailed discussion of this result, offering three reasons to account for the difference. One was that the standards of practice are not optimal. A second was that while higher pedaling rates might be optimal, rider comfort dictated a lower pedaling rate. A final reason was that the objective function does not address the force-velocity relation of muscle. Hull and Gonzalez did not argue the case for any one of the above reasons. They did note, however, that if the pedaling rate were set at 85 to 90 RPM, the rate naturally selected by cyclists generating a total power of 200W, then the crank arm length computed via the joint moment-based cost function agreed almost identically with the standard of practice. This stimulates our interest in the results of a four variable optimization with pedaling rate held constant at naturally selected rates to be discussed next.

The results of a four variable optimization while cadence is kept constant are seen in Table 4. For given cadences, four optimal variable values were computed for the three different anthropometries. Since the range of pedaling rate for typical cyclists is 90 - 105 RPM at a total power output level of 200W, the optimization was undertaken with cadences fixed at values within the range 85 - 110 RPM. From Table 4 for the average man, at 95 RPM the optimal crank arm length is 0.178m with a 2.2 percent increase in the moment cost function value compared to the value of Table 3, and at 100 RPM the optimal crank arm length is 0.167m with a 0.4 percent increase of the moment cost function value. For the short man, at 105 RPM the optimal crank arm length is 0.171m with a 0.2 percent increase in the moment cost function value. Finally, for the tall man, at 90 RPM the optimal crank arm length is 0.173m with a 2.8 percent increase in the moment cost function value.

Table 4 Four Variable Optimization for Given Cadences and Anthropometric Variations

	Short man	Average man	Tall man
Given Cadence	95 RPM	90 RPM	85 RPM
Crank arm length (L1)	0.193 m	0.191 m	0.185 m
Seat tube angle (ψ)	81.6°	78.4°	74.9°
Seat height (L5)	0.696 m	0.773 m	0.858 m
Foot position (L2i)	0.130 m	0.143 m	0.156 m
Moment cost function value	41,481 N^2m^2	48,053 N^2m^2	58,442 N^2m^2
Given Cadence	100 RPM	95 RPM	90 RPM
Crank arm length (L1)	0.182 m	0.178 m	0.173 m
Seat tube angle (ψ)	80.7°	77.6°	74.5°
Seat height (L5)	0.705 m	0.784 m	0.868 m
Foot position (L2i)	0.130 m	0.143 m	0.156 m
Moment cost function value	40,560 N^2m^2	47,982 N^2m^2	57,176 N^2m^2
Given Cadence	105 RPM	100 RPM	95 RPM
Crank arm length (L1)	0.171 m	0.167 m	0.161 m
Seat tube angle (ψ)	80.0°	77.0°	74.0°
Seat height (L5)	0.714 m	0.793 m	0.876 m
Foot position (L2i)	0.130 m	0.143 m	0.156 m
Moment cost function value	39,766 N^2m^2	47,095 N^2m^2	56,262 N^2m^2
Given Cadence	110 RPM	105 RPM	100 RPM
Crank arm length (L1)	0.161 m	0.157 m	0.151 m
Seat tube angle (ψ)	79.3°	76.5°	73.4°
Seat height (L5)	0.722 m	0.801 m	0.876 m
Foot position (L2i)	0.130 m	0.143 m	0.156 m
Moment cost function value	39,090 N^2m^2	46,405 N^2m^2	55,819 N^2m^2

These results indicate that the multivariable optimization with the moment-based cost function offers close agreement with the standard crank arm length for typically practiced cadences. As for the seat height position, the sum of the crank arm length and the seat height should be adjusted to 97 - 99 percent of the corresponding trochanteric leg length for the three different types of men. This result is the same as the five variable optimization. The seat angles are greater than the standard 73° for all three anthropometries, and the differential between anthropometries is a minimum 3°. The results suggest that the seat angle should be adjusted to the individual in order to obtain minimum

joint moments.

The results of the anthropometric analysis indicate that all five variables affect the joint moment-based cost function in cycling at constant power output. To minimize the cost function, the results imply the necessity for adjusting these variables to suit the anthropometry of individual riders. The results emphasize the importance of tailoring bicycle equipment, which bears on the biomechanics of cycling, to the anthropometry of the individual.

The results of the final stage of the analysis which was to examine the pedal force scaling method are illustrated in Figures 6a, 6b, 7a, and 7b. Figures 6a and 6b show the experimental pedal force profiles for three selected cadences (60 RPM, 90 RPM, and 120 RPM) at an average constant power of 90W (single leg). Recall that the experimental pedal force data were taken every 10 RPM for the range from 60 RPM to 120 RPM. Next, the scaled pedal force profiles are illustrated in Figures 7a and 7b. The pedal forces are scaled to the experimental pedal forces of 90 RPM (90W) which is the median cadence of the experiment.

Referring to Figures 6a, 6b, 7a, and 7b, notice that the trend of increased peak force (in an absolute sense) as pedaling rate decreases is exhibited by both scaled and experimental pedal force profiles in the downstroke region (i.e. 0° to 180°). The upstroke region (180° to 360°), however, illustrates opposite trends for scaled and experimental forces. Since the pedal forces are generally small during the upstroke hence not significantly affecting the static joint moments, it is more important to have similar trends in the downstroke region.

Because the scaled pedal force profiles did not duplicate the experimental pedal force profiles, the effect of profile type on the joint moment-based cost function was examined quantitatively. Moment cost function values for both profile types, experimental and scaled, were computed at each RPM increment in the 60 RPM to 120 RPM range and compared. For both types, the minimum cost function value was at 90 RPM. The cost function values for the experimental pedal forces from 90 RPM down to 60 RPM increased in percent deviation as did the values for the scaled forces. Cost function values for experimental pedal forces also exhibited this trend from 90 RPM to 120 RPM as did values for scaled forces. Although the percent deviation for both types of profiles increased with RPM deviation from 90 RPM, the percent deviation was consistently greater for the scaled profiles.

Despite using the constant power ergometer, recording the

experimental pedal force profiles at the desired cadence and power output level required much effort. This was because the pedal force profiles obtained experimentally were sensitive to changes in cadence, power output and pedaling style. Obtaining pedal force profiles at the 90W power level was particularly a problem at high RPM.

Overall the scaled pedal forces followed the trend of the experimental pedal forces qualitatively and quantitatively. Experimental pedal force profiles were sensitive to the variables of cycling, hence making pedal force profiles at identical power levels difficult to obtain. Accordingly the pedal force scaling method is an efficient way to create various pedal force profiles for this optimization analysis utilizing the moment-based cost function.

Conclusions

1. For a specific rider anthropometry, the variable most strongly affecting the joint moment cost function is the pedaling rate followed by the crank arm length, seat tube angle, seat height and foot position on the pedal. The sensitivities of the cost function to all four geometric variables except foot position are significant. Because the sensitivities of the crank length and two seat position variables are comparable, equal attention should be given to all three in adjusting bicycle equipment.

2. All variables interact. Accordingly, in establishing the optimal set of variable values it is important to consider them simultaneously.

3. When anthropometric parameters are varied, the optimum values of all five variables change significantly at the overall cost function minimum. In general, the crank length, seat height and foot position increase with rider height while the seat tube angle and pedaling rate decrease. These trends emphasize the importance of tailoring bicycle equipment to the individual.

4. The pedal force scaling method yields pedal force profiles which follow the same trends as those measured in the downstroke region of the crank cycle. As a result of this, the cost function also exhibits similar trends for both computed and measured pedal forces at pedaling rates both greater than and less than the optimum rate. Hence, the pedal force scaling method avoids the difficulties inherent in obtaining measured pedal force profiles without compromising the validity of results.

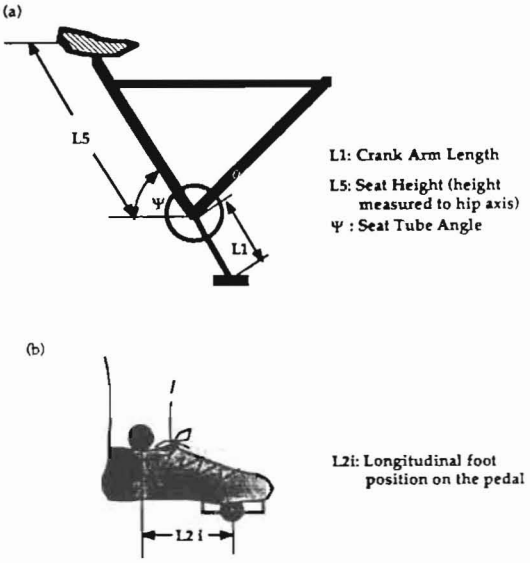

Fig. 1. Four geometric variables which can be adjusted readily in conventional cycling.

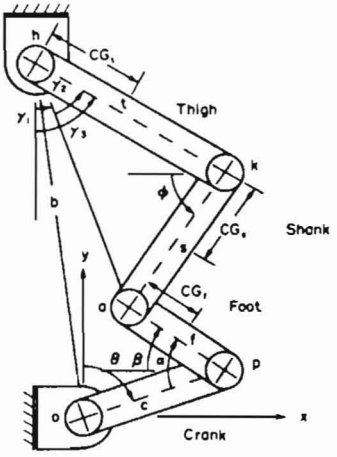

Fig. 2a. Five-bar linkage model of the bicycle-rider system. Connecting the crank and hip axes, the bicycle frame is the fifth link.

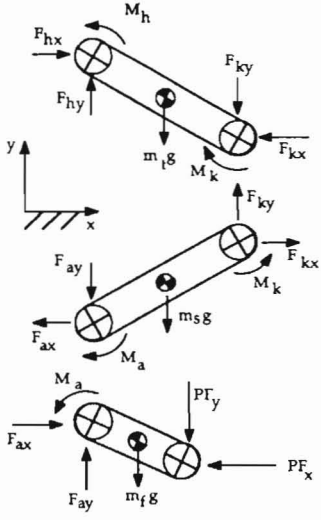

Fig. 2b. Free-body diagram of the leg for computing intersegmental loads. External loads are the horizontal (PF_x) and vertical (PF_y) pedal force components.

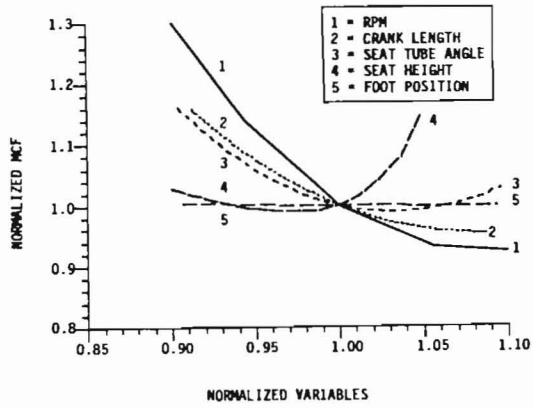

Fig. 3. Normalized variables vs. normalized moment cost function at the original reference point (RPM = 90, crank arm length = 0.170m, seat tube angle = 73°, seat height = 0.784m, foot position = 0.125m). Curves indicate relative sensitivity of the cost function to the five biomechanical variables. Sensitivity is greatest to RPM and least to foot position.

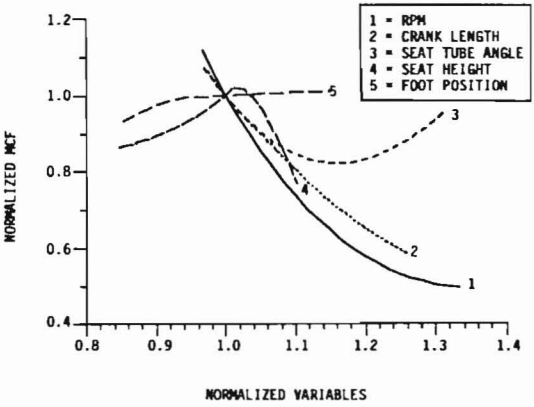

Fig. 4. Normalized variables vs. normalized moment cost function at one of the other four points (RPM = 81, crank arm length = 0.153m, seat tube angle = 66.7°, seat height = 0.784m, foot position = 0.125m). Comparison with Figure 3 shows that sensitivity remains greatest for RPM and least for foot position even though the point in five-space is different from the original reference.

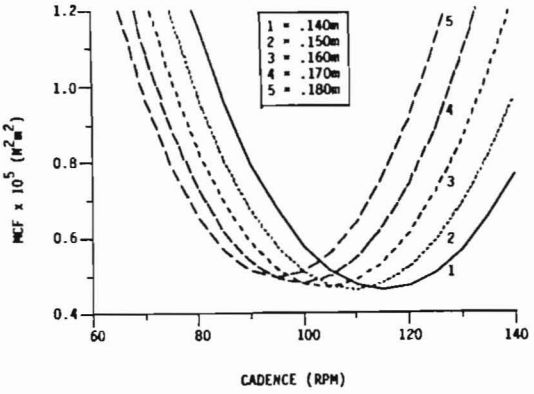

Fig. 5. Moment cost function vs. cadence for various crank arm lengths (seat tube angle = 76°, seat height = 0.804m, foot position = 0.143m). Note the increase in the cost function minimum which occurs at a crank arm length of 0.140m and pedalling rate of 115 RPM as cadence and crank arm length decrease and increase respectively.

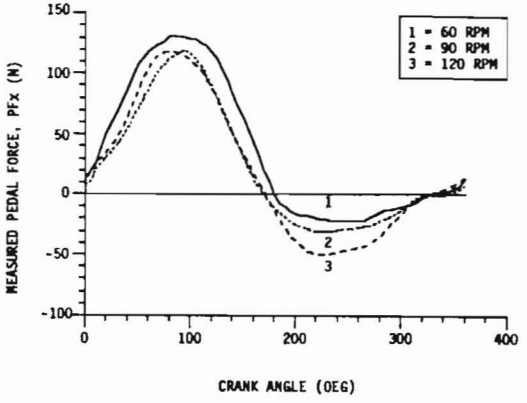

Fig. 6a. Experimental pedal forces, PFx vs. crank angle. Forces were measured using a two-load component pedal dynamometer at a constant average power output of 90 W (single leg).

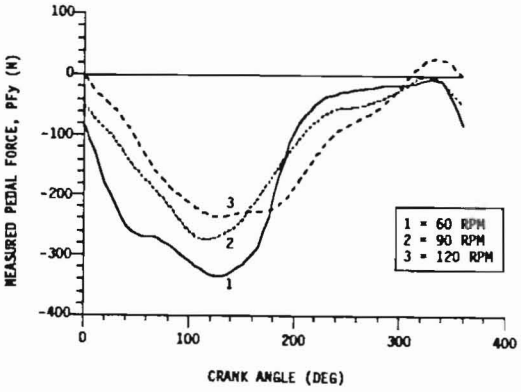

Fig. 6b. Experimental pedal forces, PFy vs. crank angle. Forces were measured using a two load component dynamometer at a constant average power output of 90 W (single leg).

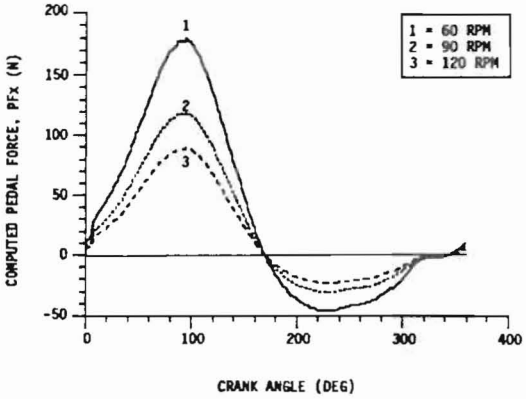

Fig. 7a. Computed pedal forces, PFx vs. crank angle (scaled to 90 RPM forces). Comparison with Figure 6a shows similar trend of peak load decreasing with increasing pedaling rate in the downstroke region (0°-180°).

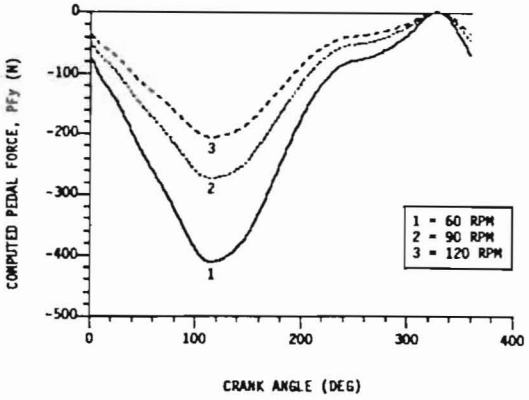

Fig. 7b. Computed pedal forces, PFy vs. crank angle (scaled to 90 RPM forces). Comparison with Figure 7a shows similar trend of absolute peak load decreasing with increasing pedaling rate in the downstroke region (0°-180°).

Acknowledgement

The authors are grateful to the U.S. Olympic Committee, and in particular to Dr. Ed Burke of the U.S. Cycling Federation, for financially supporting this research. We are also grateful to Shimano Corporation for its generous financial support and equipment donations. In this Corporation we acknowledge Shinpei Okajima (Shimano, Japan) and Wayne Stetina and John Uhte (Shimano, American). Finally, we appreciate Ms. Debbie Fowler, who ably prepared the manuscript.

References

Borysewics, E., (1985), *Bicycle Road Racing*, Velo-News Corporation, Brattleboro, Chap. 6.

Coast, J.R., and Welch, H.G., (1985), Linear Increase in Optimal Pedal Rate with Increased Power Output in Cycle Ergometry, *European Journal of Applied Physiology*, Vol. 53, No. 4, pp. 339-342.

Crowninshield, R.D. and Brand, R.A. (1981), A Physiologically Based Criterion of Muscle Force Prediction in Locomotion, *Journal of Biomechanics*, Vol. 14, No. 11, pp. 793-801.

Drillis, R. and Contini, R., (1966), Body Segment Parameters, Technical Report No. 1166.03, Vocational Rehabilitation Administration, Department of Health, Education and Welfare,New York.

Faria, I., Sjojaard, G., and Bonde-Petersen, F., (1982), Oxygen Cost During Different Pedaling Speed for Constant Power Output, *Journal of Sports and Medicine*, Vol. 22, pp. 295-299.

Hamley, J.M. and Thomas, V., (1967), Physiological and Postural Factors in the Calibration of the Bicycle Ergometer, *Journal of Physiology (London)*, Vol. 191, pp. 55-57.

Harrison, J. Y., (1970), Maximizing Human Power Output by Suitable Selection of Motion Cycle and Load, *Human Factors*, Vol. 12, No. 3, pp. 315-329.

Hull, M.L. and Gonzalez, H.K. (1988), Bivariate Optimization of Pedaling Rate and Crank Arm Length in Cycling, to appear in the *Journal of Biomechanics*.

Hull, M.L., Gonzalez, H.K. and Redfield, R., (1988), Optimization of Pedaling Rate in Cycling Using a Muscle Stress-Based Objective Function, *International Journal of Sport Biomechanics*, Vol. 4, No. 1, pp. 1-20.

Hull, M.L. and Jorge, M., (1985), A Method for Biomechanical Analysis of Bicycle Pedaling, *Journal of Biomechanics*, Vol. 18, No. 9, pp. 631-644.

Miller, N.R. and Ross, D.J. (1980), The Design of Variable Ratio Chain Drives for Bicycles and Ergometers - Application to a Maximum Power Bicycle Drive, *Proceedings to International Conference on Medical Devices and Sports Equipment*, ASME, New York, pp. 49-56.

Newmiller, J. and Hull, M.L., (1986), A Mechanically Decoupled Two Force Component Bicycle Pedal Dynamometer, to appear in the *Journal of Biomechanics*.

Nordeen-Snyder, K.S., (1977), The Effect of Bicycle Seat Height V ariation Upon Oxygen Consumption and Lower Limb Kinematics, *Medicine and Science in Sports*, Vol. 9, No. 2, pp. 113-117.

Pierre, D.A., (1969), *Optimization Theory with Applications*, John Wiley and Sons, New York, Chapter 6.

Redfield, R. and Hull, M.L. (1986a), On the Relation Between Joint Moments and Pedaling Rates at Constant Power in Cycling, *Journal of Biomechanics*, Vol. 19, No. 4, pp. 317-

329.
Redfield, R. and Hull, M.L. (1986b), Prediction of Pedal Forces in Bicycling Using Optimization Methods, *Journal of Biomechanics*, Vol. 19, No. 7, pp. 523-540.
Seabury, J.J., Adams, W.C., and Ramey, M.R., (1977), Influence of Pedaling Rate and Power Output on 'Energy Expenditure During Bicycle Ergometry, *Ergonomics*, Vol. 20, No. 5, pp. 491-498.
Wells, K.F. and Luttugens, K., (1976), *Kinesiology*, W. B. Saunders Co., Philadelphia.
Whitt, F.R. and Wilson, D.G., (1982), *Bicycling Science*, MIT Press, Cambridge, MA.